Mineralogic reaction zones at a calc-silicate/metapelite interface: an example of trace element mobility in a metamorphic environment

J. V. Owen and J. Dostal

Department of Geology, Saint Mary's University, Halifax, N.S., Canada B3H 3C3

and

B. N. Church

Department of Energy, Mines and Petroleum Resources, Victoria, B.C., Canada V8V 1X4

Abstract

Metasomatic interaction on a cm scale between calc-silicate pods and the enclosing sillimanite + biotite + tourmaline gneiss at Partridge Breast Lake, northern Manitoba, Canada, led to the development of an inner (by calc-silicate rock), hornblende-rich reaction zone and an outer, biotite-rich zone. The boundary between the reaction zones is interpreted as the original calc-silicate/metapelite interface. Compared with its metapelitic protolith, the biotite zone shows a two- to twenty-fold depletion in the concentrations of incompatible trace elements (notably the light rare earths, U, Th, Nb, Ta, Zr and Hf). In contrast, the relative concentrations of trace elements remained nearly constant during the mineralogical transformation of the calc-silicate rock to the hornblende zone. The depletion of trace elements in the biotite zone is attributed to the dissolution of accessory phases (e.g. monazite). Although stable at the metamorphic conditions (~600–650°C at ~4.5 kbar) prevalent during metasomatism, Mg-rich tourmaline is absent in the biotite zone, suggesting that either the pH or composition (e.g. the (Al + Si)/(Ca + Mg + Fe) ratio) of the aqueous fluid phase was inappropriate for the preservation of this mineral.

Keywords: metasomatism, reaction zone, calc-silicate, metapelite, trace element, Manitoba.

Introduction

The metasomatic transfer of mobile components across lithological boundaries can produce reaction zones that are mineralogically distinct compared with contiguous rock layers. Notable examples include the formation of single or multiple reaction zones between metapelite and amphibolite or calc-silicate rocks (henceforth, 'calc-silicate').

The mineralogy of the reaction zones depends on (1) the mineralogy and bulk composition of the original rock layers; (2) metamorphic conditions (pressure, temperature, and fluid composition); and (3) the solubility of protolith phases and the mobility of their constituent components in the metamorphic fluid. For example, biotite ± garnet can form during small-scale, potassic metasomatism of amphibolite enclosed by pelitic gneiss (Owen, 1993), whereas garnet + orthoamphibole can form in instances where K is removed from amphibolite (Tuisku, 1992). Even if mineralogically-distinct reaction zones are absent, variations in whole-rock element ratios can indicate that some geochemical trends are not primary, but reflect secondary processes such as metasomatism (Nicholls *et al.*, 1991). Metasomatic alteration typically involves relatively soluble (i.e. 'mobile') components such as the alkalis and related trace elements. Although a pore fluid is crucial to their development (by promoting ionic diffusion), reaction zones can form in the absence of a μ_{H_2O} gradient (Vander Auwerea, 1993).

Mineralogical Magazine, June 1994, Vol. 58, pp. 205–214

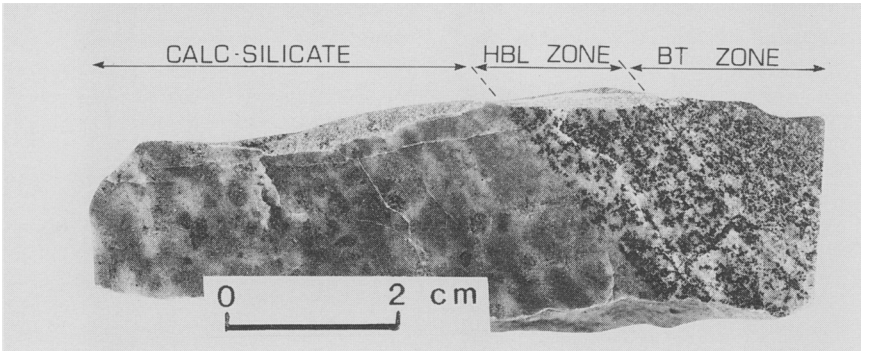

FIG. 1. Photograph of the analysed calc-silicate rock and hornblende and biotite-rich reaction zones. The contiguous metapelite, detached near the edge of the biotite zone illustrated here, is not shown.

This paper reports on the mineralogical and bulk compositional changes associated with the formation of narrow (2–4 cm total width), double reaction-zones (Fig. 1) at the interface between calc-silicate 'pods' within sillimanite gneiss of Proterozoic age at Partridge Breast Lake (~57°20′N, 97°50′W), northern Manitoba (Kretz, 1959, 1967; Moore *et al.*, 1960). This occurrence is unusual because some incompatible trace elements, including high field strength (HFS) elements (e.g. Zr, Hf, Nb, Ta), radioelements (U, Th), and the light rare earths (*LREE*), show extreme (two- to twenty-fold) depletion in part of the reaction zone, compared with its inferred metamorphic precursor (i.e. the contiguous rock layer). These elements are generally considered to be relatively immobile during metamorphism, but their concentrations can vary in cases where: (1) metamorphic fluids are capable of dissolving host phases (typically accessory minerals like apatite, zircon or monazite) and transporting their constituent components, which then are ultimately introduced into suitably reactive rocks and precipitated in discrete minerals or on grain boundaries; or (2) other components are removed (or added) during fluid flux, thereby concentrating (or depleting) the rock in less soluble components. The latter process is commonly associated with extreme fluid fluxes in ductile shear zones, which can undergo volume losses of up to at least 60% via dissolution mechanisms that commonly promote massive desilicification (e.g. O'Hara and Blackburn, 1989; Selverstone *et al.*, 1991), thereby enriching the rock in relatively insoluble components. Comparatively few cases (e.g. Grauch, 1989) have been described where *HFSE* and the *LREE* have become depleted during metamorphism or deformation.

The depletion of these 'immobile' elements in part of the reaction zone described here therefore may result from either the dissolution during metasomatism of phases in which these components reside, or the preferential enrichment of parts of the reaction zone in other components. These hypotheses are tested using composition–volume relationships and mass-balance calculations.

Field occurrence and mineralogy

Multiple polished thin-sections of a calc-silicate pod, its metapelitic host rock, and the intervening reaction zones were prepared for modal and microprobe analyses. Modes were estimated by point counting thin-sections. Phase compositions (Table 1) were determined with a JEOL Superprobe 733 equipped with four wavelength-dispersive spectrometers and one energy-dispersive spectrometer, and operated with a beam current of 15 kV and 10 nA.

The calc-silicate occurs as lozenge-shaped 'pods' up to 0.6 m long within sillimanite + K feldspar-bearing pelitic gneiss. The calc-silicate contains quartz (~28 vol.%), diopside (~35%), plagioclase (~28%), garnet (~3–5%), titanite (~2–4%) and Fe(Ti) oxides (~2%), and is enclosed by mineralogically distinct reaction zones. Plagioclase in the calc-silicate is nearly pure anorthite (An_{97}) (Table 1).

Biotite is the principal ferromagnesian phase in the metapelite. The biotite has an intermediate Mg/(Mg + Fe) ratio (X_{Mg} = 0.43). Xenomorphic muscovite partially encloses fibrolite mats that form 2–8 mm long bundles elongated parallel to the biotite schistosity. In the same rock, however, subidiomorphic muscovite porphyroblasts are

TABLE 1. Microprobe analyses of selected silicate phases from calc-silicate pods, pelitic gneiss, and intervening reaction zones.

	Calc-silicate				Hornblende zone				Biotite zone								Metapelite			
									Fine-grained				Medium-grained							
	Cpx	Grt		Pl	Hbl	Grt		Pl	Bt	Grt		Pl	Bt	Grt		Pl	Bt	Msc	Tur	Pl
		core	rim			core	rim			core	rim			core	rim					
SiO_2 (wt.%)	50.82	37.27	37.37	43.15	49.25	37.44	37.26	43.24	36.05	37.39	37.22	45.02	35.99	37.66	37.33	44.25	34.59	46.11	35.68	57.83
TiO_2	0.07				0.41				2.89				2.28				2.19	0.41	0.53	
Al_2O_3	0.42	21.21	21.23	37.25	5.87	21.16	21.28	36.85	16.79	21.47	21.39	36.51	16.85	21.58	21.61	35.50	20.51	36.95	35.47	26.59
FeO	17.75	19.61	21.59		18.70	22.80	23.66		19.46	27.24	25.08		19.11	28.52	28.10		20.08	1.23	6.51	
MnO	1.33	8.42	7.95		0.69	7.39	8.23		0.29	8.55	9.51		0.20	5.56	7.77					
MgO	7.40	0.58	0.85		10.94	1.44	1.46		11.23	2.71	2.20		11.82	3.10	2.63		8.35	0.73	6.12	
CaO	23.50	14.21	12.10	20.66	11.87	11.03	9.31	20.54	0.20	4.72	5.22	19.57		5.35	4.47	19.52			1.07	8.35
Na_2O	0.06			0.32	0.41			0.43	0.24			0.81	0.19			1.01		0.44	1.55	6.79
K_2O					0.22				8.90				8.76			0.28	9.29	9.45		0.18
Total	101.35	101.30	101.09	101.38	98.36	101.26	101.20	101.06	96.05	102.08	100.62	101.91	95.20	101.77	101.91	100.56	95.01	95.32	86.93	99.74
X_{Mg}	0.426				0.510				0.507				0.524				0.426		0.626	
X_{An}^{Pl}				0.973				0.964				0.930				0.900				0.400
Garnet																				
X_{Mg}		0.022	0.032			0.055	0.056			0.103	0.087			0.119	0.101					
X_{Fe}		0.414	0.463			0.485	0.509			0.582	0.553			0.613	0.606					
X_{Ca}		0.384	0.332			0.301	0.256			0.129	0.148			0.147	0.123					
X_{Mn}		0.180	0.173			0.159	0.179			0.185	0.213			0.121	0.170					

seen to contain trails of fine sillimanite needles, suggesting that at least two generations of aluminosilicate and white mica are present. Some samples contain prismatic sillimanite that overprints biotite and muscovite. The K-feldspar (microcline) is riddled with idiomorphic, S-fabric-forming biotite that also occurs as a matrix phase. Plagioclase (An_{40}) is subordinate to microcline. Green tourmaline, a conspicuous minor phase (~1–3 vol.%), is compositionally-intermediate between dravite and schorl (i.e. X_{Mg} = 0.63; Table 1). Zircon and apatite are accessory phases. Garnet is absent.

The calc-silicate pods are separated from the metapelite by a double reaction-zone comprising an inner, hornblende-rich zone, and an outer, biotite-rich zone. The hornblende zone contains actinolitic hornblende (~31 vol.%), quartz (~30%), anorthite (An_{97}; ~24%), essentially unzoned garnet ($Pyr_6Alm_{50}Grs_{28}Sps_{16}$; ~9%), titanite (~3%), Fe oxide (~2%), and accessory zircon and apatite. The hornblende and garnet form 1 mm poikiloblasts that enclose quartz, plagioclase and/or titanite.

The inner part of the biotite zone contains quartz (~40 vol.%), biotite (X_{Mg} = 0.5; ~25%), anorthite (An_{92}; ~35%), poikilitic garnet ($Pyr_{10}Alm_{58}Grs_{13}Sps_{19}$; 0–3%) that encloses biotite, quartz, titanite, Fe oxide and/or zircon. The outer part of this zone is relatively biotite-rich, and can be somewhat coarser grained (biotites to 1 mm; garnets to 1 cm). It contains quartz (~18 vol.%), biotite (X_{Mg} = 0.5; ~36%), and anorthite (An_{90}; ~45%). Large poikilitic garnets ($Pyr_{11}Alm_{61}Grs_{14}Sps_{15}$; ~1 vol.%) are compositionally similar to the finer grained garnet in the inner part of the biotite zone.

The identity of accessory and minor phases in the reaction zones and host rocks is important, because these minerals tend to control the distribution of various trace elements. Titanite is characteristic of the calcic lithologies (calc-silicate; hornblende zone). Although diagnostic of the metapelite, tourmaline is absent in the biotite zone.

Metamorphic conditions

Metamorphic temperature (T) conditions prevalent during formation of the reaction zones can be estimated from the composition of garnet-biotite and garnet-hornblende pairs for a pressure (P) value constrained by coexisting clinopyroxene–garnet–plagioclase in the quartz-bearing calc-silicate pods. The P-sensitivity of the calc-silicate assemblage is based on the net-transfer reaction:

3 diopside + 3 anorthite = 2 grossular + pyrope + 3 quartz

which incorporates a T-sensitive Mg–Fe exchange reaction between clinopyroxene and garnet. Because of the elevated spessartine (~17 mol.%) and low pyrope (~3%) contents of the garnet, the composition of this assemblage falls outside the guidelines for direct calibrations of this geothermobarometer (e.g. Newton, 1983). consequently, we have estimated P and T for the calc-silicate using the TWQ software of Berman (1991), which uses an internally-consistent thermodynamic database (Berman, 1988) and recent activity–composition models (e.g. garnet: Berman (1990), Berman and Koziol (1991); biotite: McMullin *et al.* (1991), plagioclase: Fuhrman and Lindsley (1988); clinopyroxene: ideal two-site mixing model (Newton, 1983)) to calculate multi-equilibrium phase diagrams for specified mineral assemblages.

TWQ yields P–T values of 4 kbar, 600°C using garnet core compositions, and 4.5 kbar, 670°C using rims. The rim compositions of garnet coexisting with biotite in fine- and medium-grained parts of the biotite zone indicate a T of 580°C (at 4.5 kbar); core compositions give higher temperatures of 620 and 640°C, respectively. The temperatures determined using calc-silicate garnet rim compositions are incompatible with the results of reaction zone Grt–Bt thermometry. This indicates that, in the reaction zone, garnet rims re-equilibrated with the biotite-rich matrix during cooling. Garnet-amphibole thermometry of the hornblende zone yields similar results. Equilibria between garnet and calcic amphibole endmembers yield a range of temperatures (510–585°C at 4.5 kbar) using garnet cores; rim compositions yield slightly lower temperatures (490–570°C). We conclude that the reaction zones formed at conditions of ~600–650°c and ~4.5 kbar.

Geochemistry

Bulk rock samples of the calc-silicate, metapelite and both reaction zones were analysed for their major, trace and rare earth concentrations. Major elements were determined by X-ray fluorescence wavelength-dispersive analysis of fused pellets. The rare earths, Th, Ta, Zr, and Hf were determined by ICP-MS after Na sintering (Longerich *et al.*, 1990). The other trace elements (Table 2) were determined by ICP-MS after acid dissolution.

The sillimanite gneiss is a typical metapelite, with $K_2O \gg Na_2O$, elevated Al_2O_3 (21.8 wt.%), and a low CaO content (0.24%). The calc-silicate is aluminous (Al_2O_3 = 14.8 wt.%), alkali-poor

TABLE 2. Major and trace element concentrations in altered calc-silicate pods from Partridge Breast Lake, Manitoba.

	Calc-Silicate	Amphibole zone	Biotite zone	Sillimanite gneiss
SiO_2 (wt.%)	60.00	62.31	49.66	58.71
TiO_2	0.59	0.79	1.10	0.70
Al_2O_3	14.80	14.01	18.24	21.80
Fe_2O_3(t)	5.41	6.98	12.69	7.51
MnO	0.63	0.64	0.28	0.06
MgO	1.76	2.80	5.88	2.82
CaO	12.81	9.19	2.98	0.24
Na_2O	0.28	0.21	0.58	0.40
K_2O	0.19	0.33	5.90	5.19
P_2O_5	0.24	0.32	0.23	0.10
L.O.I.	0.58	0.70	2.50	1.40
Total	97.29	98.28	100.04	98.93
Rb (ppm)	7	11	294	232
Cs	0.49	0.58	13.15	5.71
Ba	20	32	10.37	1156
Sr	456	217	98	59
Tl	0.03	0.04	1.43	1.10
Li	10.59	15.73	139.30	35.07
Ta	1.24	1.93	0.31	1.44
Nb	14.8	17.1	4.7	16.5
Hf	6.15	9.09	1.71	2.50
Zr	235	357	67	90
Y	43	66	22	24
Th	15.68	21.92	0.81	21.36
U	2.98	4.50	0.56	4.88
La	47.92	69.69	6.01	52.10
Ce	98.33	154.26	14.38	105.30
Pr	10.90	16.66	2.05	11.84
Nd	42.32	64.00	9.73	42.93
Sm	7.67	12.99	2.68	7.62
Eu	1.60	1.85	0.67	1.15
Gd	7.27	12.60	3.55	5.98
Tb	1.06	1.88	0.59	0.85
Dy	7.46	12.87	4.16	5.27
Ho	1.46	2.41	0.84	0.96
Er	4.31	6.79	2.45	2.72
Tm	0.65	0.99	0.35	0.41
Yb	4.14	6.25	2.29	2.61
Lu	0.60	0.94	0.36	0.42
Mg#	36.58	44.27	47.85	42.65
ρ	2.91	2.88	2.89	2.76

(Na_2O + K_2O ~ 0.5%), and MgO (1.8%) is subordinate to Fe_2O_3(t) (5.4%).

Compared to the metapelite, the biotite zone is enriched (in absolute terms) in Ca and Mn, whereas the hornblende zone is enriched in K relative to the calc-silicate. To a certain extent, the biotite and hornblende zones thus represent complementary zones of depletion and enrichment, wherein some components apparently migrated in opposite directions across the calc-silicate/metapelite interface during metamorphism, and contributed to the stabilization of new or compositionally-distinct phases in the reaction zones (e.g. anorthite in the biotite zone). There is, however, striking evidence for open-system behaviour shown by other components in

the biotite zone, which is depleted in silica, the *LREE*, and other incompatible trace elements relative to both the calc-silicate and metapelite.

The calc-silicate and sillimanite gneiss have chondrite-normalized *REE* patterns (Fig. 2) similar to average continental crust (Taylor and McLennan, 1985), and show pronounced *LREE* enrichment. Both rocks have overlapping *LREE* (La to Sm), and flat heavy rare earth (*HREE*) patterns (Gd to Lu), but the La/Yb ratio (~12) of the calc-silicate is significantly lower than that of the gneiss (La/Yb ~20). The hornblende zone has a similar *REE* pattern to that of calc-silicate. Both rocks have similar La/Yb ratios, but the hornblende zone is characterized by higher total *REE* abundances, and a more pronounced negative Eu anomaly (Fig. 2). In contrast, the sillimanite gneiss and biotite zone show similar patterns only for the heaviest rare earths (Ho to Lu). The biotite zone is progressively depleted in the light rare earths (e.g. La/Yb ~2.6), such that La concentrations are nearly tenfold higher in the metapelite.

Protoliths

Composition-volume and mass balance relationships require that the lithologic precursor(s) of the reaction zone material be identified. This in turn requires consideration of where the calc-silicate/metapelite boundary was originally positioned.

The boundary between multiple reaction zones in metasomatic systems can represent either the original (pre-alteration) lithological interface, or a reaction boundary. The reaction zones have widely divergent mineralogies and bulk compositions that are more closely allied with their respective, adjacent lithologies. For example, the calc-silicate and amphibole zone are CaO-rich, K_2O-poor rocks; the converse is true for the biotite zone and metapelite (Table 2). This suggests that the interface separating the hornblende and biotite zones is a compositional boundary corresponding to the original margin of the calc-silicate pod, across which fluids derived from both rock types interacted during metamorphism.

Composition–volume and mass balance relations

The bulk compositional data reveal that the biotite zone is depleted in several trace elements that are generally considered to be immobile during metamorphism and metasomatism. This does not necessarily imply that any or all of these components were mobile during interaction between the calc-silicate and pelitic gneiss, but

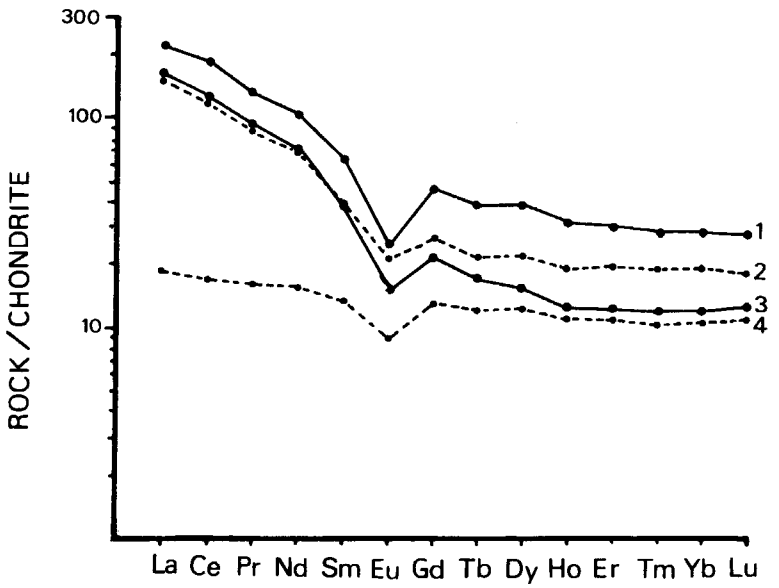

FIG. 2. Chondrite-normalized *REE* plot of (1) the hornblende zone (2) calc-silicate, (3) metapelite, and (4) the biotite zone.

only that their concentrations have apparently decreased relative to other components. Such apparent concentration changes only have meaning if expressed relative to a specified reference frame, and can be quantified by taking into account composition–volume relationships between the reaction zones and their inferred protoliths.

Composition–volume relationships proposed by Gresens (1967) have been applied widely in the petrological literature (e.g. Dipple *et al.*, 1990; Selverstone *et al.*, 1991). Grant (1986) expressed Gresens' (1967) composition–volume equations as linear relationships that compare the concentrations of various components in the protolith and its altered equivalent. These relationships can be solved graphically by plotting the concentration of various components in the altered rock against their concentration in the inferred protolith. Minor and trace element concentrations are scaled to avoid the clustering of points near the origin of the plot. Linear arrays of points constitute an isocon, a line of equal elemental concentration, which has a slope equal to the concentration of isocon components in the altered rock (C_i^a) divided by their concentration in the protolith (C_i^o). Concentration changes can be expressed relative to model isocons (based on constant mass, volume or a chosen 'immobile' element) or to a best-fit isocon defined by a linear array of points that passes through the origin in $C_i^o - C_i^a$ space.

Components delineating a best-fit isocon were not necessarily immobile (relative to an external reference frame) during metasomatism, but, if mobile, they showed the same sense and relative magnitude of mobility, so that ratios of their concentrations are similar in both the altered rock and its protolith.

Component abundances in the reaction zones and their inferred precursors are shown in Fig. 3. The two reaction zones show strikingly different patterns on these plots. Data for the hornblende zone delineate a conspicuous best-fit isocon defined by a wide variety of *HFSE* and *REE* (Fig. 3A). This isocon has a slope of 1.48, corresponding to a mass loss of −33% and a volume loss of −32%, which can be accounted for by substantial decreases (relative to 'immobile' trace elements) in SiO_2, CaO, Al_2O_3 and Fe_2O_3. Using the compositional and density data in Table 2, and the metasomatic volume change inferred from the best-fit isocon, the hornblende zone can be related to the calc-silicate by the following balanced expression:

100 g calc-silicate − 18.4 g SiO_2 − 6.7 g CaO − 5.5 g Al_2O_3 − 0.8 g Fe_2O_3 − 0.2 g MnO − 0.1 g Na_2O − 0.1 g TiO_2 + 0.1 g MgO = 67 g Hbl zone

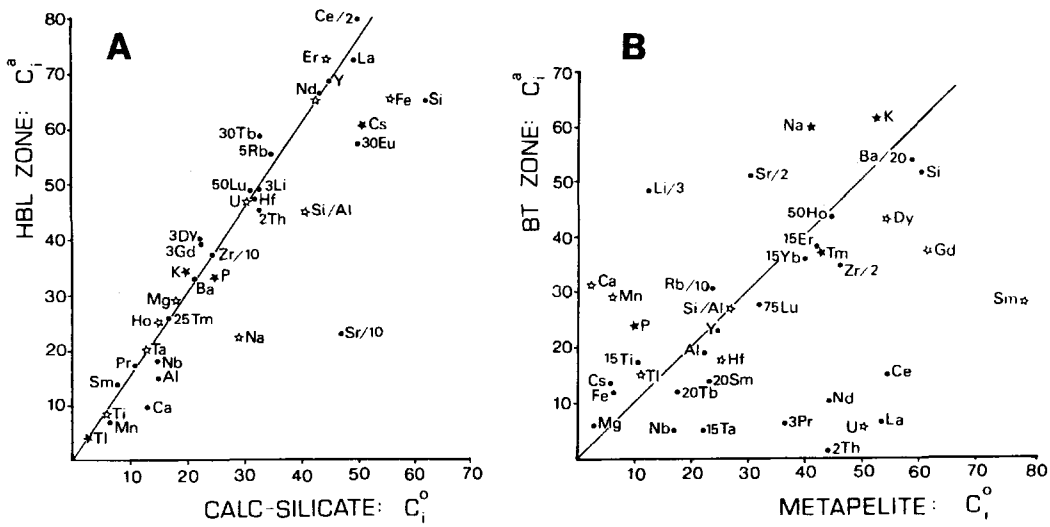

FIG. 3. Element abundance plots comparing (A) the hornblende zone and the calc-silicate, and (B) the biotite zone and the metapelite. Data were normalized to 100% anhydrous before plotting, and are scaled as indicated (dots). Other scaling factors vary with symbol: closed stars (× 100), open stars (× 10). Data for major element oxides are flagged as cations (e.g. Al for Al_2O_3).

It is important to note that an isocon based on major element data for this sample (e.g. constant Al_2O_3) would correspond more closely to the constant mass isocon (i.e. a line equating scales on the isocon diagram), but would indicate the enrichment of relatively insoluble trace elements (e.g. the *REE*) in the altered rock.

Data for the biotite zone display a relatively scattered pattern, and there is no obvious best-fit isocon (Fig. 3B). However, the SiO_2/Al_2O_3 ratios of the biotite zone (= 2.69) and metapelite (= 2.72) are similar despite contrasts in their respective plagioclase compositions. This suggests that, although liberated during dissolution of feldspars (and other aluminous silicates), SiO_2 and Al_2O_3 were either immobile, or showed the same degree of mobility during metamorphism. The ratio of these components therefore constitutes a suitable reference frame for evaluating volume and component-concentration changes between the reaction zones and their protoliths. The constant SiO_2/Al_2O_3 isocon is nearly coincident with the constant mass isocon. It has a slope of 1.011, corresponding to a volume change of −4%. Relative to this isocon, this reaction zone is enriched in Ca, Na and P, and in components associated with biotite (K, Ti, Mg, Fe, Cs, Li). It is depleted in *REE* (especially the *LREE*) and *HFSE*.

The metapelite is related to the biotite zone by the following balanced expression based on the presumed constancy of SiO_2/Al_2O_3:

100 g metapelite − 7.2 g SiO_2 − 2.9 g Al_2O_3 + 5.6 g Fe_2O_3(t) + 3.3 g MgO + 2.8 g CaO + 0.9 g K_2O + 0.4 g TiO_2 + 0.2 g MnO + 0.2 g Na_2O + 0.1 g P_2O_5 = 99 g biotite zone

Composition–volume relations show that geochemical contrasts between the biotite zone and the metapelite are not due to differential volume changes during metasomatism. Rather, the depletion of various trace elements in the biotite zone is likely to be due to the destabilization of phases that controlled the distribution of these components.

Significance of trace element depletion in the biotite zone

The systematic depletion of ostensibly 'immobile' trace elements in the biotite zone points to the dissolution of the phase(s) in the metapelite that controlled the distribution of *HFSE* and *LREE*. Although some of these components tend to be concentrated in apatite and zircon, these phases occur in both the metapelite and the biotite zone, precluding the possibility that either mineral is responsible for the trace element signature of the biotite zone. This conclusion is supported by the higher concentration of P in the biotite zone, and by the relatively minor (compared with other *HFSE*) depletion of Zr in this zone relative to the metapelite.

Clearly another phase — one that is restricted to the metapelite — must be responsible for the trace element characteristics of the biotite zone. Tourmaline is an obvious candidate. Several workers have shown that tourmaline strongly fractionates *LREE* relative to *HREE*, and also has an affinity for the *HFSE*, but *REE* concentrations can vary by 4 orders of magnitude depending on the host rock. For example, La concentrations in schorls from pegmatites can vary from 0.01–50 times chondritic values (Jolliff *et al.*, 1987), to 750 times chondrites for tourmalines in granites (Neiva, 1974). Furthermore, *REE*-depleted tourmalines (*LREE* < chondrites) tend to show positive chondrite-normalized Eu anomalies, whereas *REE*-enriched tourmalines have negative Eu anomalies (Jolliff *et al.*, 1987). It is apparent that tourmaline dissolution may account for some of the trace element differences between the biotite zone and its precursor. Analysis of the tourmaline by laser ablation microprobe-inductively coupled plasma-mass spectrometry (LAM-ICP-MS; Jackson *et al.*, 1992) reveals, however, that the concentrations of trace elements in this mineral are insufficient to account for the massive depletion of the *LREE* and *HFSE* in the biotite zone. For example, La concentrations are consistently < 5 p.p.m., and Ce varies between 7 and 10 p.p.m. The *HREE*, Th and Ta are near or below detection limit (i.e. < 3 p.p.m.). Uranium and Zr are also present in low concentrations (< 10 p.p.m.), but locally (μm scale) reach hundreds of p.p.m. in some tourmalines. The existence in this mineral of subdomains anomalously enriched in (e.g.) U or Zr suggests the presence of trace element or (more likely) inclusion-rich zones. In either case, these data show that the dissolution of tourmaline cannot be directly responsible for the depletion of various trace elements in the biotite zone, but that this feature is likely to be related, at least in part, to the degradation of minute (submicron) inclusions of different accessory phases that controlled the distribution of various trace elements.

The identity of these accessory phases remains problematic, but is constrained by the trace elements depleted in this reaction zone. The strong depletion of *LREE* relative to *HREE* and of Th relative to U and Y is consistent with the dissolution of monazite despite higher concentrations of P, which would be buffered by the

presence of apatite. Minute inclusions of accessory phases are especially susceptible to degradation when the host phase dissolves; in the case of monazite, dissolution would be promoted by elevated water activities (e.g. Rapp and Watson, 1986). However, the depletion of Nb, Ta, Zr and Hf in the biotite zone requires the dissolution of an additional accessory phase(s) which is likely to include that apparently detected during LAM-ICP-MS analysis of tourmaline.

The conspicuous absence of tourmaline in the biotite zone sheds light on the composition of the fluid phase in which these various 'immobile' components were soluble. Experimental data for synthetic dravite (Vorbach, 1989) reveals that Mg tourmaline is stable at the $P-T$ conditions ($\sim$600–650°C at 4.5 kbar) determined for the reaction-zone samples described here. Consequently, the metasomatic fluid phase must have been compositionally distinct from the fluid accompanying the earlier metamorphic event responsible for the stabilization of tourmaline in the metapelite. Although the composition of fluids accompanying the formation of metamorphic tourmalines is poorly known (Vorbach, 1989), experimental data reveal that tourmaline is favoured by weakly alkaline, aqueous solutions enriched in B, and with a high proportion of Al+Si to Ca+Mg+Fe (Deer *et al.*, 1986). No whole-rock analytical data for B are available, but it is plausible that the enrichment of the biotite zone in Ca, Mg and Fe (for a given SiO_2/Al_2O_3 ratio; Fig. 3B) could account for the destabilization of tourmaline in the protolith. Alternatively, tourmaline would have been unstable if the metasomatic fluid was acidic or strongly alkaline (Deer *et al.*, 1986).

Conclusions

Geochemical interaction between calc-silicate and sillimanite-grade metapelite at Partridge Breast Lake led to the development of reaction zones showing contrasting degrees of compositional divergence from their respective precursors. Apart from desilification, the loss of Ca and Na, and minor potassic alteration, the hornblende zone was derived by relatively isochemical metamorphism of the calc-silicate, particularly with regard to the relative concentrations of trace elements. In contrast, the biotite zone shows massive depletions in various trace elements (notably the *LREE*, Th, U, Ta, Nb, Hf, Zr) as well as a loss of Si and a gain of K, P, Ca and femic components (Mg, Fe). The increases in K and Ca in the hornblende and biotite zones, respectively, indicate the transfer of these (and related) components in opposite directions across the calc-silicate/metapelite interface during metasomatism. The depletion of the altered metapelite in relatively immobile trace elements is attributed to the dissolution of minute accessory phases, some of which apparently resided in essential silicate phases, including tourmaline. Dravitic tourmaline is stable at the metamorphic conditions ($\sim$600°C at 4–5 kbar) prevalent during metasomatism, so it is likely that the dissolution of this phase either reflects unsuitably low(?) pH of the fluid phase, or the bulk increase in the altered metapelite of Ca and femic components.

Acknowledgements

Analytical data acquisition was funded through individual NSERC operating grants to Owen and Dostal. David Pass did the point-counting. We thank Simon Jackson for analysing tourmaline by LAM-ICP-MS. The paper benefited from comments by an anonymous referee.

References

Berman, R. G. (1988) Internally-consistent thermodynamic data for stoichiometric minerals in the system Na_2O–K_2O–CaO–FeO–Fe_2O_3–Al_2O_3–SiO_2–TiO_2–H_2O–CO_2. *J. Petrol.* **29**, 445–522.

Berman, R. G. (1990) Mixing properties of Ca–Mg–Fe–Mn garnets. *Amer. Mineral.* **75**, 328–44.

Berman, R. G. (1991) Thermobarometry using multi-equilibrium calculations: a new technique, with petrological applications. *Can. Mineral.*, **29**, 833–55.

Berman, R. G. and Koziol, A. M. (1991) Ternary excess properties of grossular–pyrope–almandine garnets and their influence in geothermobarometry. *Amer. Mineral.*, **76**, 1223–31.

Deer, W. A., Howie, R. A. and Zussman, J. (1986) *Rock-forming Minerals. Vol. 1B. Disilicates and Ring Silicates.* Longman Scientific & Technical, Harlow, U.K. 2nd ed. 629 pp.

Dipple, G. M., Wintsch, R. P. and Andrews, M. S. (1990) Identification of the scales of differential element mobility in a ductile fault zone. *J. Metamorph. Geol.*, **8**, 645–61.

Fuhrman, M. L. and Lindsley, D. H. (1988) Ternary-feldspar modelling and thermometry. *Amer. Mineral.* **73.**, 201–15.

Grant, J. A. (1986) The isocon diagram — a simple solution to Gresens' equation for metasomatic alteration. *Econ. Geol.*, **81**, 1976–82.

Grauch, R. I. (1989) Rare earth elements in metamorphic rocks. In *Geochemistry and Mineralogy of Rare Earth Elements.* (Lipin, B. R. and

McKay, G. A., eds.), Mineralogical Society of America, Reviews in Mineralogy, v. **21**, 147–67.

Gresens, R. L. (1967) Composition–volume relationships of metasomatism. *Chem. Geol.*, **2**, 47–65.

Jackson, S. E., Longerich, H. P., Dunning, G. R. and Fryer, B. J. (1992) The application of laser-ablation microprobe-inductively coupled plasma-mass spectrometry (LAM-ICP-MS) to *in situ* trace-element determinations in minerals. *Can. Mineral.*, **30**, 1049–64

Jolliff, B. L., Papike, J. J. and Laul, J. C. (1987) Mineral recorders of pegmatite internal evolution: *REE* contents of tourmaline from the Bob Ingersoll pegmatite, South Dakota. *Geochim. Cosmochim. Acta*, **51**, 2225–32.

Kretz, R. (1959) Geology of Northern Indian Lake area, Manitoba. *Geol. Surv. Can.*, Map 2-1959.

Kretz, R. (1967) Granite and pegmatite studies at Northern Indian Lake, Manitoba. *Geol. Surv. Can. Bull.*, **148**, 42 pp.

Longerich, H. P., Jenner, G. A., Fryer, B. J. and Jackson, S. E. (1990) Inductively coupled plasma-mass spectrometric analysis of geological samples: A critical evaluattion based on case studies. *Chem. Geol.*, **83**, 105–18

McMullin, D., Berman, R. G. and Greenwood, H. J. (1991) Calibration of the SGAM thermobarometer for pelitic rocks using data from phase equilibrium experiments and natural assemblages. *Can. Mineral.*, **29**, 889–908.

Moore, J. M., Jr., Hart, S. R., Barnett, C. C. and Hurley, P. M. (1960) Potassium-argon ages in northern Manitoba. *Bull. Geol. Soc. Amer.* **71**, 225–30.

Neiva, A. M. R. (1974) Geochemistry of tourmaline (schorlite) from granites, aplites and pegmatites from northern Portugal. *Geochim. Cosmochim. Acta*, **38**, 1307–17.

Newton, R. C. (1983) Geobarometry of high-grade metamorphic rocks. *Amer. J. Sci.*, **283A**, 1–28.

Nicholls, J., Stout, M. Z. and Ghent, E. D. (1991) Characterization of partly-open-system chemical variations in clinopyroxene amphibolite boudins, Three Valley Gap, British Columbia, using Thompson space calculations. *Can. Mineral.*, **29**, 633–53.

O'Hara, K. and Blackburn, W. H. (1989) Volume-loss model for trace element enrichments in mylonites. *Geology*, **17**, 524–7.

Owen, J. V. (1993) Syn-metamorphic element transfer across lithological boundaries in the Port-aux-Basques gneiss complex, Newfoundland. *Lithos*, **29**, 217–33.

Rapp, R. P. and Watson, E. B. (1986) Monazite solubility and dissolution kinetics: implications for the thorium and light rare earth chemistry of felsic magmas. *Contrib. Mineral. Petrol.*, **94**, 304–16.

Selverstone, J., Morteani, G. and Staude, J.-M. (1991) Fluid channelling during ductile shearing: transformation of granodiorite into aluminous schist in the Tauern Window, Eastern Alps. *J. Metamorph. Geol.*, **9**, 419–31.

Taylor, S. R. and McLennan, S. M. (1985) *The Continental Crust: its Composition and Evolution.* Blackwell, Oxford, U.K.

Tuisku, P. (1992) Contact zone interaction of metabasites with metapelites: Amphibolite facies mineral assemblages, chemical profiles and their origin, the Puolankajarvi Formation, Finland. *Lithos*, **27**, 279–300.

Vander Auwera, J. (1993) Diffusion controlled growth of pyroxene-bearing margins on amphibolite bands in the granulite facies of Rogaland (Southwestern Norway): implications for granulite formation. *Contrib. Mineral. Petrol.*, **114**, 203–20.

Vorbach, A. (1989) Experimental examinations on the stability of synthetic tourmalines in temperatures from 250°C to 750°C and pressures up to 4 kb. *Neues Jarhb. Mineral. Abh.*, **161**, 69–83.

[*Manuscript received 7 September 1993: revised 14 October 1993*]